Radial force modeling for bearingless motors based on analyze of field origins

Blaise Lapôtre[a], Noureddine Takorabet[a], Farid Meilbody-Tabar[a], Ramdane Lateb[b], Joaquim Da Silva[b]

[a] Université de Lorraine, GREEN, 2 av. de la forêt de Haye, 54516 Vandœuvre-lès-Nancy, France, Blaise.lapotre@univ-lorraine.fr
[b] SKF Magnetic Mechatronics 2 rue des champs, 27250 Saint Marcel, France

***Abstract*— This paper proposes a global harmonic analysis of a multiphase bearingless PM-motor topology to determine the radial force by considering normal and tangential field components. This allows establishing the semi-analytical expressions of the radial force considering the location of field origin. The accuracy of the model is verified by full FEM model using a statistic approach. The semi-analytic model allows predicting the force waveforms according t the stator-rotor topology. The analysis of two specific topologies is performed and highlights the origin of force ripples. The fastness of this semi-analytical model makes it suitable to implement in a design optimization process.**

A. Introduction

In the last decade, high speed motors and active magnetic bearings have been widely used in high pure or wear-free applications. One challenging solution is to use bearingless motors, providing both functions, torque as well as levitation force generation with the same machine.

The principle of bearingless motors has been adapted for different motor topologies: PM motor [1], reluctance machine [2] or induction motor [3]. The main idea consists in creating levitation forces by using two consecutive field space harmonics of ranks p and $p+1$ [4]. The field is either created by windings or magnets according to the adopted motor topology.

Several techniques have been developed to determine the radial forces in electric machines. In the particular case of bearingless motors many authors have proposed interesting contributions for different topologies. For toothless machines the Lorentz force can be considered [5]. Another way consists in using magnetic co-energy method to evaluate the forces [2]. An alternate approach is to use the Maxwell stress tensor method in the air gap [6].

The analytical calculation of radial forces and torque in bearingless machines is quite complex when field harmonics should be taken into account. In some cases, it is possible to assume some assumptions to make the calculation easier. Some authors have proposed to neglect the tangential component of the field in the air-gap [7]. This approach is appropriate for small air-gap machines and when normal component of the field is dominant. This is the case of induction machines or variable reluctance machines [2].

Other authors prefer eliminate directly the harmonic by winding configuration or topology but without consideration presumed parasitic force norm or direction of [8-9].

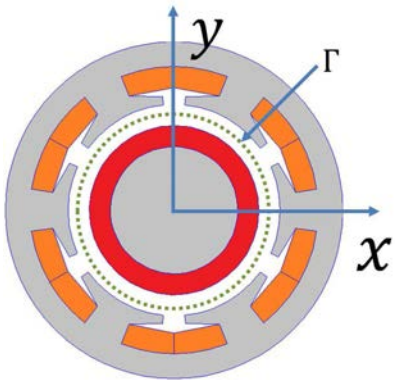

Figure 1 : Six slot bearingless motor geometries

Under other conditions we can establish an analytical model with a large number of adjustable parameters [10] or with utilization of force calculated by Maxwell stress tensor and Lorenz force [11].

In this paper, the authors propose an analytical model based on the spectral decomposition of the fields created by different sources (stator winding, rotor magnets, ...). The calculation of the forces is performed by using the Maxwell stress tensor expressed in terms of different harmonics of the normal and tangential components of the flux density in the air-gap. In order to simplify the expressions and reduce the number of parameters, the magnetic vector potential formulation has been introduced. This approach allows evaluating the contribution of each couple of consecutive harmonics to the total levitation force. Thus, the design process of these machines is made more straightforward and easier.

B. Radial force formulation

As mentioned above [4], the radial force components of bearingless motor are resulting from the interaction of magnetic consecutive field space harmonics of ranks p and $p+1$. Using Maxwell tensor method on contour Γ figure 1, the projection of the force components in two axes (x, y) fixe relative to the stator are given in equation (1):

$$F_x = \frac{r.L_z}{2\mu_0}\int_0^{2\pi}[(B_n^2 - B_t^2)\cos\theta_s - 2B_tB_n\sin\theta_s]d\theta_s$$
$$F_y = \frac{r.L_z}{2\mu_0}\int_0^{2\pi}[(B_n^2 - B_t^2)\sin\theta_s + 2B_tB_n\cos\theta_s]d\theta_s \quad (1)$$

B_n and B_t are respectively the normal and tangential components of the air gap flux density. With L_z , r respectively, the iron length and the radius in the middle of the air-gap, θ_s is the angular coordinate of an arbitrary point on the considered contour and μ_0 is the permeability of vacuum.

Using Fourier transformation, normal and tangential components of the flux density can be expressed as follows:

$$\begin{cases} B_{n\varrho}(\theta_{n\varrho},\theta_s) = \frac{1}{2}\sum_k \left|Bn_{\varrho,k}\right| e^{j\theta_{n\varrho,k}} e^{jk\theta_s} + \left|Bn_{\varrho,k}\right| e^{-j\theta_{n\varrho,k}} e^{-jk\theta_s} \\ B_{t\varrho}(\theta_{t\varrho},\theta_s) = \frac{1}{2}\sum_k \left|Bt_{\varrho,k}\right| e^{j\theta_{t\varrho,k}} e^{jk\theta_s} + \left|Bt_{\varrho,k}\right| e^{-j\theta_{t\varrho,k}} e^{-jk\theta_s} \end{cases} \quad (2)$$

The subscript ϱ indicates the nature of the considered field source which can be either permanent magnets or the current distributions.

$\left|Bn_{\varrho,k}\right|$ and $\left|Bt_{\varrho,k}\right|$ are the amplitudes of the k[th] harmonics of the normal and tangential components of the air-gap flux density. $\theta_{n\varrho,k}$ and $\theta_{t\varrho,k}$ are their phases.

By neglecting the saturation of the iron core, the superposition principle can be applied. The combination of equations (1) and (2) allows determining the components F_x and F_y of the force which can then be expressed by:

$$\begin{cases} F_x = \frac{r.L_z\pi}{2\mu_0} \sum_{\varrho,\varsigma,k} FX_{k,\varrho,\varsigma} \\ F_y = \frac{r.L_z\pi}{2\mu_0} \sum_{\varrho,\varsigma,k} FY_{k,\varrho,\varsigma} \end{cases} \quad (3)$$

The components $FX_{k,\varrho,\varsigma}$ and $FY_{k,\varrho,\varsigma}$ are the elementary forces generated by the interaction of two successive harmonics of rank k and k+1 of the flux density given in (2) due to the same source or different ones ϱ, ς.

$$\begin{aligned} FX_{k,\varrho\varsigma} = {} & \left|B_{n\varrho,i}B_{n\varsigma,i+1}\right| cos(\theta_{n\varrho,i} - \theta_{n\varsigma,i+1}) \\ & - \left|B_{t\varrho,i}B_{t\varsigma,i+1}\right| cos(\theta_{t\varrho,i} - \theta_{t\varsigma,i+1}) \\ & - \left|B_{n\varrho,i}B_{t\varsigma,i+1}\right| sin(\theta_{n\varrho,i} - \theta_{t\varsigma,i+1}) \\ & - \left|B_{t\varrho,i}B_{n\varsigma,i+1}\right| sin(\theta_{t\varrho,i} - \theta_{n\varsigma,i+1}) \end{aligned} \quad (4)$$

$$\begin{aligned} FY_{k,\varrho\varsigma} = {} & \left|B_{n\varrho,i}B_{n\varsigma,i+1}\right| \sin(\theta_{n\varrho,i} - \theta_{n\varsigma,i+1}) \\ & - \left|B_{t\varrho,i}B_{t\varsigma,i+1}\right| \sin(\theta_{t\varrho,i} - \theta_{t\varsigma,i+1}) \\ & + \left|B_{n\varrho,i}B_{t\varsigma,i+1}\right| \cos(\theta_{n\varrho,i} - \theta_{t\varsigma,i+1}) \\ & + \left|B_{t\varrho,i}B_{n\varsigma,i+1}\right| \cos(\theta_{t\varrho,i} - \theta_{n\varsigma,i+1}) \end{aligned} \quad (5)$$

The subscripts ϱ and ς denote the nature of the considered field sources which can be either permanent magnets or the current source.

The main idea is to reduce the number of parameter in equations (4) and (5). By considering the magnetic vector potential MVP A on the contour Γ, the Fourier decomposition of this potential is:

$$A_\varrho = \frac{1}{2}\sum_k A_{\varrho,k} e^{ik\theta_s} + A^*_{\varrho,k} e^{-ik\theta_s} \quad (6)$$

where

$$A_{\varrho,k} = \left|A_{\varrho,k}\right| e^{i\theta_{\alpha,k}} \quad (7)$$

By the derivation of potential the tangential and normal component are given by:

$$\begin{aligned} B_{n\varrho} = \frac{1}{r}\frac{\partial A}{\partial \theta_s} = {} & \frac{1}{2}\frac{1}{r}\sum_k k\left|A_{\varrho,k}\right| e^{i\left(\theta_{\varrho,k}+\frac{\pi}{2}\right)} e^{ik\theta_s} \\ & + k\left|A_{\varrho,k}\right| e^{-i\left(\theta_{\varrho,k}+\frac{\pi}{2}\right)} e^{-ik\theta_s} \end{aligned} \quad (8)$$

and

$$\begin{aligned} B_{t\varrho} = -\frac{\partial A}{\partial r} = \sum_k {} & -\frac{\partial\left|A_{\varrho,k}\right|}{\partial r} e^{i\theta_{\varrho,k}} e^{ik\theta_s} \\ & -\frac{\partial\left|A_{\varrho,k}\right|}{\partial r} e^{-i\theta_{\varrho,k}} e^{-ik\theta_s} \end{aligned} \quad (9)$$

By identification is possible two establish a relationship between tangential and normal field phase. Depending on the sign of $\partial|A_{\varrho,k}|/\partial r$ two cases are possible:

- $\theta_{\varrho t,k} = \theta_{\varrho n,k} - \frac{\pi}{2}$ when $\partial|A_{\varrho,k}|/\partial r$ are positive, the field source is located outside the air gaps contour
- $\theta_{\varrho t,k} = \theta_{\varrho n,k} + \frac{\pi}{2}$ when $\partial|A_{\varrho,k}|/\partial r$ are negative, in this case the field source is located inside the air gaps contour.

Introducing the phase relationship given above in both equations (4) and (5), $FX_{i,\varrho\varsigma}$ and $FY_{i,\varrho\varsigma}$ can be simplified as follows:

$$\begin{cases} FX_{i,\varrho\varsigma} = K\, cos\left(\theta_{n\varrho,i} - \theta_{n\varsigma,i+1}\right) \\ FY_{i,\varrho\varsigma} = K\, sin\left(\theta_{n\varrho,i} - \theta_{n\varsigma,i+1}\right) \end{cases} \quad (10)$$

The expression of the coefficient K depends on the location of the field sources with respect to the contour: inside the contour or outside the contour. The four possible cases are summarized in Table I.

The expressions given in Table I show the impact of different field space harmonics on the mean value or the harmonics of the radial force. This can be used for improving the design of bearingless motor. Illustrative examples will be given in the following sections.

TABLE I COEFFIENT (K) EXPRESSIONS

	$B_{i,\varrho external}$	$B_{i,\varrho internal}$
$B_{i+1,\varsigma external}$	$\left(\left\|B_{n\varsigma,i+1}\right\| + \left\|B_{t\varsigma,i+1}\right\|\right).\left(\left\|B_{n\varrho,i}\right\| - \left\|B_{t\varrho,i}\right\|\right)$	$\left(\left\|B_{n\varsigma,i+1}\right\| + \left\|B_{t\varsigma,i+1}\right\|\right).\left(\left\|B_{n\varrho,i}\right\| + \left\|B_{t\varrho,i}\right\|\right)$
$B_{i+1,\varsigma internal}$	$\left(\left\|B_{n\varsigma,i+1}\right\| - \left\|B_{t\varsigma,i+1}\right\|\right).\left(\left\|B_{n\varrho,i}\right\| - \left\|B_{t\varrho,i}\right\|\right)$	$\left(\left\|B_{n\varsigma,i+1}\right\| - \left\|B_{t\varsigma,i+1}\right\|\right).\left(\left\|B_{n\varrho,i}\right\| + \left\|B_{t\varrho,i}\right\|\right)$

C. determination of harmonic evolution

N-phase, 2-pole Permanent Magnet motor is considered. The stator winding is composed of n concentrated coils, one coil for one tooth.

The stator phase currents (i_j; j=1 to n) is the superposition of two n-phase current systems (I1 and I2) defined by.

$$\begin{cases} i_{j,1} = I_1 \cos\left(\omega_1 t + \phi_1 + \dfrac{(j-1)\pi}{n}\right) \\ i_{j,2} = I_2 \cos\left(\omega_2 t + \phi_2 + \dfrac{2(j-1)\pi}{n}\right) \end{cases} \quad (11)$$

In the general case, I_1, I_2, ω_1, ω_2, ϕ_1, and ϕ_2 represent the amplitudes, frequencies and the phases of the two systems respectively.

The current system I1 generates a 2-pole magnetomotive force (mmf) and the current system I2 generates a 4-pole mmf.

According to the multiphase winding theory, the two n-phase systems I1 and I2 generate forward harmonics of the air-gap flux density of ranks $nm+1$ and $nm+2$ and backward harmonics of ranks $nm-1$ and $nm-2$.

The phase angles of these space harmonic depend directly of current phase for forward harmonics the evolution are in same way while the evolution are reverse for backward harmonic

As well as the norm of every harmonic have a linear dependence to the current norm.

$$\begin{cases} |Bn_{\varrho,k}| = K_{n,k}.I_\varrho & \theta_{n\varrho,k} = \theta_{0n\varrho,k} \pm \omega_\varrho t \\ |Bt_{\varrho,k}| = K_{t,k}.I_\varrho & \theta_{t\varrho,k} = \theta_{0t\varrho,k} \pm \omega_\varrho t \end{cases} \quad (12)$$

The magnets create a radial flux density which harmonic spectrum depends on the size of the magnets and the nature of the magnetization. If the slot effect is neglected the amplitudes of the flux density harmonic are constant while their phases increase linearly with the speed of the rotor and the harmonic rank (13).

$$\begin{cases} |Bn_{m,k}| = Cst & \theta_{nm,k} = \theta_{0nm,k} + k\omega t \\ |Bt_{m,k}| = Cst & \theta_{tm,k} = \theta_{0tm,k} + k\omega t \end{cases} \quad (13)$$

These considerations can estimate the flux density and determine the force for any position of rotor and current configuration by performing only one FE calculation for each field sources.

D. validation of model by statistic analyses

In order to validate the developed model, it is necessary to test it on a large number of machines whose geometrical parameters Figure 2 vary in a 5-D space corresponding to geometrical parameters and for different scenarios of operation.

The 5-D space of parameters is presented in Table II which gives the upper and lower bounds of each geometrical parameter.

The different scenarios of operation are summarized in Table III. They concern mainly the values of the currents, their phases and the rotor position.

The number of geometric and electrical parameters leads to a 10-D space. Therefore a statistical approach comparing FE and semi-analytical results is adopted. It consists in randomizing a machine and an operating point and computing their performances with both models. The comparison is focused on the radial forces determined by Maxwell stress tensor in the air-gap. This process is performed on 1000 machines randomly chosen in the 10-D space.

TABLE II INTERVAL OF TOPOLOGY VARIABLES

Parameter	Interval
Slot and phase number	5 or 6
Stator inner radius R_a	10 at 40 mm
Air gap e	1 at 3mm
Thickness of magnet a	1 at 5 mm
Slot opening λ	0% to 33 %

TABLE III INTERVAL OF ELECTRICAL VARIABLES

Parameter	Interval
Rotor position	0 to 2π rad
Norm of current system I1 : I_1	0 to 400 At
Phase of current system I1 : Φ_1	0 to 2π rad
Norm of current system I2 : I_2	50 to 550 At
Phase of current system I2 : Φ_2	0 to 2π rad

The relative errors between forces computed by the two methods are calculated in terms of norm and direction. Figure 3 shows the corresponding histogram of the errors which have Gaussian distributions.

For the direction of the force, the errors do not exceed ±1.5°. The evaluation of normal distribution gives a mean value of -0.002° with a variance of 0.011°. For the norm of the force, the errors is less than 5% and the normal distribution is characterized by a mean value of 0.4% and variance of 0.062%.

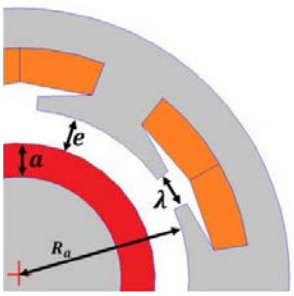

Figure 2 : Representation of topology variable

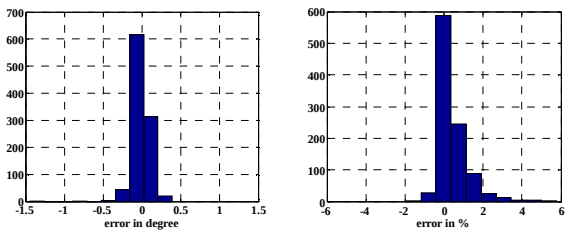

(a) (b)

Figure 3 : (a) histogram of angle error in direction of force between semi analytical model and FEM (b)histogram of relative norm error of force between semi analytical model and FEM

These two results allow validating this statistical approach in terms of size of population (1000). Consequently, the proposed semi-analytical model is validated by means of full FE calculation.

E. Example of a bearingless 6 phase PM-motor

We consider a 6-phase, 2-pole permanent magnet motor. The stator winding is composed of 6 concentrated coils considered like external sources of field. The rotor is composing of one magnet ring with radial or diametrical magnetization Figure 4.

Their configuration create harmonic of flux density in air-gap depending on their sources (magnet , system current I1 and I2) according to equation (12) and (13) these existing harmonics and their frequencies are summarized in Table IV and V. In this tables we find the different pairs of harmonics which interact and generate radial force components. They can be gathered in three groups highlighted with the three colors (red, blue, green) shown in Table IV and V. They correspond also to the different cases listed in Table I:

- red: force component which norm is the product of two sums,
- blue: forces component which norm is the product of two subtractions,
- green: forces which norm is product of subtraction and sum.

Case of parallel magnetized rotor :

The Table IV allows highlighting the interactions between the different field harmonics. The general form of the elementary force due to a couple of field harmonics of generate by currents is given as bellow:

$$K\cos(\omega_1 t - \omega_2 t + \phi) \qquad (14)$$

where ϕ is the shift phase between the two field harmonics.

The interaction between the fields generated by the magnets and the currents can be resumed in one interaction of 2 first harmonic with equation:

$$K\cos(\omega t - \omega_2 t + \phi) \qquad (15)$$

It should be reminded that to have a constant torque, the electric pulsation of the system I1 and the mechanical pulsation must be equal $\omega = \omega_1$ (the rotor has one pole pair,

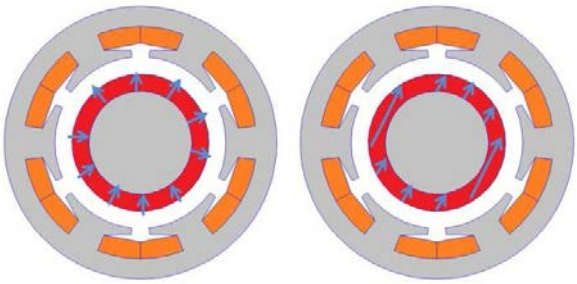

(a) Radial (b) Parallel

Figure 4 : Magnetization topologies of the rotor

Table IV). In addition, to obtain a constant levitation force it is necessary to have $\omega_1 = \omega_2$ (equ. 13). Figure 5 Shows the force components F_x and F_y obtained by the proposed semi-analytical model with the 16 first harmonics and by a full FEM computation. There is an excellent accordance between the two models; then the semi-analytical model is perfectly validated for parallel magnetized rotors.

Case of radial magnetized rotor :

As mentioned above Radially magnetized rotor generates flux density in the air-gap with odd space harmonics of frequencies $(2m+1)\omega$. These field harmonics interact with the field harmonics generated by the current system I2 which are shown in red and blue in Table V. The general form of the elementary forces due to a couple of field harmonics is in the following form:

$$K\cos(\mp(2m+1)\omega t \mp \omega_2 t + \phi) \qquad (16)$$

On Figure 6, we show the F_x and F_y component of the levitation force obtained in the case of radial magnetized rotor As in the case of parallel magnetized rotor, the mechanical pulsation and the electrical pulsation of the current system I_2 must be equal to $\omega = \omega_1 = \omega_2$. In this condition, contrary to the case of parallel magnetized rotor, the levitation force has not only a constant component, it contains also the harmonics as of frequency $2m\omega$.

TABLE IV HARMONIC PULSATIONS FOR 6 PHASE AND RADIAL (IN READ) OR PARALLEL MAGNTIZATION

Root field	Space harmonium								
	1	2	3	4	5	6	7	8	9
I1	ω_1				$-\omega_1$		ω_1		
I2		ω_2		$-\omega_2$				ω_2	
Magnet	ω								

TABLE V HARMONIC PULSATIONS FOR 6 PHASE AND RADIAL (IN READ) OR PARALLEL MAGNTIZATION

Root field	Space harmonium								
	1	2	3	4	5	6	7	8	9
I1	ω_1				$-\omega_1$		ω_1		
I2		ω_2		$-\omega_2$				ω_2	
Magnet	ω		3ω		5ω		7ω		9ω

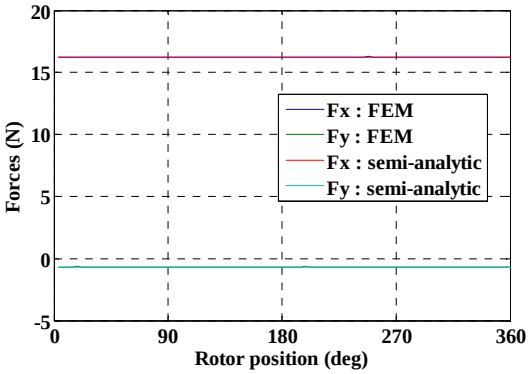

Figure 5 : Force x-y components of the studied six-phase motor with parallel magnetization

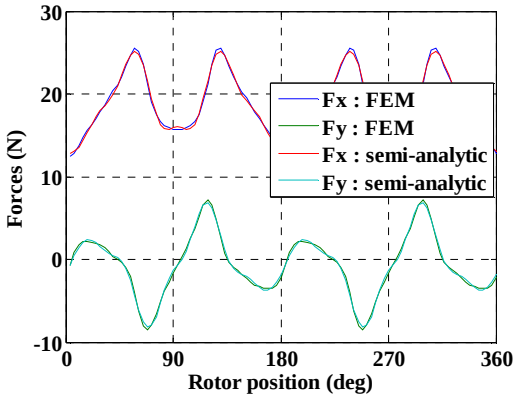

Figure 6 : Force x-y components of the studied six-phase motor with radial magnetization

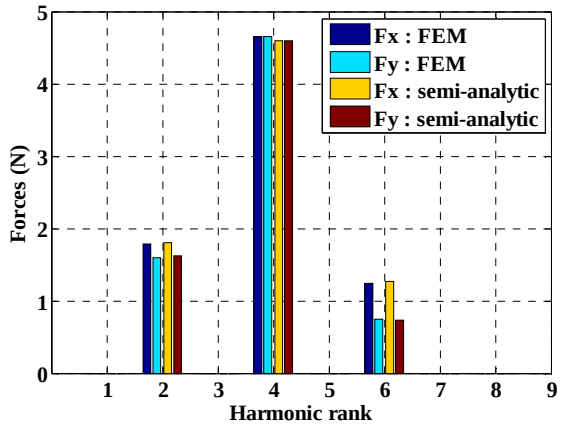

Figure 7 : Force harmonic analysis for radial magnetization

by using both analytical model with 16 first harmonics and full FEM computations. In this case also there is an excellent agreement between the results obtained by these two models.

The spectral analysis of the forces waveforms is shown on Figure 7 for both F_x and $F_y$components. This spectral analysis allows the identification of the interaction between the different harmonics of the flux density. For example, the 2nd harmonic of the force is produced by the interaction of the 2nd field harmonic generated by the current system I2 and the 3rd field harmonic generated by the magnets. In order to indicate the mentioned field harmonics interaction we use henceforth the following notation $(2_{I2}, 3_{mag} \Rightarrow 2_{force})$.

The interaction $(4_{I2}, 3_{mag} \Rightarrow 4_{force})$ corresponds to the red group characterized by the product of two sums (Table I) while the interaction $(2_{I2}, 3_{mag} \Rightarrow 2_{force})$ corresponds to the blue group characterized by the product of two subtractions (Table I). That's why the amplitude of the 4th harmonic of the force is higher than the amplitude of its 2nd harmonic.

Furthermore, it can be seen that the force harmonics of higher ranks may have several origins. For example the interactions $(4_{I2}, 5_{mag} \Rightarrow 6_{force})$ and $(8_{I2}, 7_{mag} \Rightarrow 6_{force})$ lead to the 6th harmonic of force. These harmonics are weak because they are generated by high rank field harmonics which have low amplitudes.

F. CPU time considerations

In the proposed semi-analytic model, the determination of radial force is performed in two steps:

- The first step consists in calculating the air-gap flux density and its Fourier decomposition for each source (magnet and current systems I1 and I2). This is performed once and requires only 3 FE calculations. This step needs fixed time called initialization.
- The second step consists to compute the force for a given instant (time) t_k. Using equations (12) and (13), the air-gap flux density is reconstituted for the considered instant and the force components are calculate by equations (10) and Table I. This is performed for each instant and does not require FE calculations. This step needs variable time depending on the number of considered instants.

For example in the machine considered in the previous section, the number of nodes us fixed to 7000 node and the calculations are performed with a processor Intel core i7-3740 (2.7GHz). The first step takes 9.3 seconds and the calculation of the forces one point in the second step need 1 millisecond. For 100 points over a mechanical period the proposed semi analytical model takes less than 10 seconds while the full FE method takes 235seconds.

The CPU time is strongly reduced with the proposed model which can be used in optimization processes or in coupled models of control on Matlab-Simulink platforms.

G. Conclusion

In this paper, the authors present a new approach for modeling of radial forces in bearingless machines. The model is based on the spectral decomposition of the flux density distribution in the air-gap, generated by different sources (magnets in rotor and currents in stator). The spectral formulation of the radial force is performed with Maxwell stress tensor. It allows the calculation of the different interaction between the field harmonics and predicts the harmonic content of the force waveforms. Such model is

useful for the designer which may specify the undesirable field harmonics before starting the design.

This model needs few FEM calculations and consequently it is very fast compared to full FEM computations.

REFERENCES

[1] M. Oshima, S. Miyazawa, T. Deido, A. Chiba, F. Nakamura, T. Fukao, "Charactreristics of a permanent magnet type bearingless motor*", IEEE trasactions on industry application*, vol. 32, no. 2, pp. 363–370, 1996.

[2] A. Chiba, M. Azizur Rahman, T. Fukao, "Radial force in a bearingless reluctance motor" *IEEE transactions on magnetics*,vol 27,no 2, pp. 786–790, 1991.

[3] M. Kang, J. Huang, J. Yang, H. Jiang, "Analysis and experiment of a 6 phase bearingless induction motor", *Proceedings on Electrical Machines and Systems. ICEMS*, pp. 990–994, 2008.

[4] Y. Okada, S. Miyamoto, T. Ohishi, "Levitation and torque control of internal permanent magnet type bearingless motor," *IEEE transaction on control systems technology* , vol. 4, no. 5, pp. 565-571, 1996.

[5] D. Steinert, T. Nussbaumer, J. Kolar "Concept of a 150 krpm bearingless slotless disc drive with combined windings'', *Proceedings on Electric Machines & Drives Conference, IEMDC,* pp. 311–318, 2013

[6] G. Munteanu, A. Binder, T. Schneider, "Loss measurement of a 40 kw high-speed bearingless PM synchronous motors'', *Proceedings on Energy Conversion Congress and Exposition, ECCE,*, pp. 722–729, 2011,

[7] S. Serri, A. Tani, G. Serra, "Analytical model of radial forces considering mutual effects between torque and levitation current space vectors in 5-phase PM bearingless motors'', *Proceedings on Industrial Electronics Society, IECON* , pp. 5142–5147, 2013

[8] T. Schneider, J. Petersen, G. Serra, "Influence of pole pair combinations on high-speed bearingless permanent magnet motor performance'', *Proceedings on Power Electronics, Machines and Drives, PEMD.*, pp. 707–711, 2008

[9] B. Li, J. Huang, W. Kong, L. Zhao, "Analysis of Half-coiled Short-pitch Windings with Different Phase Belt for Multiphase Bearingless Motor'', *Journal of Electrical Engineering & Technology, vol 9 No1* pp. 162–168, 2014

[10] G. Munteanu, A. Binder, T Schneider, B. Funieru, "No-load tests of a 40 kW high-speed bearingless permanent magnet synchronous motor'', *Proceedings of* International Symposium on *Power Electronics Electrical Drives Automation and Motion,* SPEEDAM, Pisa, Italy, pp 1460-1465, 2010

[11] F. Zürcher, T. Nussbaumer, J.W. Kolar, "Principles of magnetic levitation force and motor torque generation by superposition of harmonics in bearingless brushless motors'', *Proceedings on Industrial Electronics,. IECON '09*, pp. 1246–1251, 2009